Indirect nuclear spin-spin interactions in PbTe

R. C. Patnaik
Department of Physics, Khallikote College, Berhampur 760 001, Orissa, India

R. L. Hota
Condensed Matter Theory Group, National Physical Laboratory, Dr. K. S. Krishnan Road, New Delhi 110 012, India and Department of Physics, Jagannath Institute for Technology and Management, Paralakhemundi 761206, Orissa, India

G. S. Tripathi
Department of Physics, Berhampur University, Berhampur 760 007, Orissa, India

(Received 14 August 1997)

We make a careful analysis of various contributions to the indirect ^{207}Pb nuclear spin-spin interactions $A_{jj'}$ in PbTe. The calculation takes into account all three hyperfine interactions and includes both the intraband and the interband contributions within a $\mathbf{k}\cdot\boldsymbol{\pi}$ formalism. The relativistic effects are considered through the double group basis wave functions and energy levels around the energy gap. We calculate $A_{jj'}$ from three different contributions: (a) a full valence band and an empty conduction band, (b) electrons in n-type PbTe, and (c) holes in p-type PbTe. In the first case the coupling tensor is quite appreciable and changes from ferromagnetic (FM) order to antiferromagnetic (AFM) order as the internuclear separation R increases. In the case of full band contribution all of the hyperfine interactions are found to be important. The carrier contributions are calculated in each case for two typical carrier (both electron and hole) densities. In the case of p-type PbTe, $A_{jj'}$ is isotropic and due mainly to contact hyperfine interactions. The noncontact interactions arising out of mixing of bands, albeit weak, are also taken into account. In the case of n-type PbTe the noncontact hyperfine interactions, namely, the orbital and the dipolar interactions, are important and the coupling constant is anisotropic. The coupling constants calculated for carrier densities of the order of 10^{18} cm^{-3} are found to be about four orders less than the corresponding value in metallic lead. Although there are no experimental results for comparison, the order of magnitude appears to be reasonable in view of the low density of carriers considered, as compared to the metallic density. Furthermore, in the absence of any other theoretical work in the case of semiconductors in general and in PbTe in particular, the present work furnishes valuable information regarding the nature of hyperfine interactions and their relative contributions to the indirect nuclear spin-spin interaction in PbTe. Some of the systematics of our calculation agree with those predicted in the case of indirect exchange interaction involving magnetic impurities in PbTe. [S0163-1829(98)04328-8]

I. INTRODUCTION

Indirect nuclear spin-spin interactions, dominated by the isotropic Ruderman-Kittel (RK) interaction[1] and the anisotropic pseudo-dipolar (PD) interaction[2] have been investigated thoroughly in metals[3–7] during the past three decades. The subject became more important after the discovery of the nuclear magnetic ordering in copper at about 25 nk and in silver at about 2 nk.[8] These interactions furnish valuable information about the electronic structure and the nature of the electronic wave functions in metals, apart from explaining the nuclear magnetic resonance (NMR) linewidth measurements and the electron-nuclear hyperfine interactions in them. Relative strengths of many-body and relativistic effects can also be ascertained from the calculations of RK and PD interactions. An exhaustive review of the subject for metals has been made in the work of Oja and Lounasmaa.[9]

Although, as mentioned above, the study of hyperfine interactions and related properties can be found in abundance in metals, these properties have not been studied with such fervour and enthusiasm in semiconductors. It is due partly to the fact that the observation of such effects in semiconductors is difficult in view of the relatively smaller density of carriers and partly to the extremely difficult calculations required to incorporate both the intraband and the interband contributions across the band gap.

Recently one of the authors derived a theory for the indirect nuclear interactions including both spin-orbit and many-body effects.[10] The theory also included all the electron-nuclear hyperfine interactions—contact, orbital, and dipolar. While in metals the contact interaction is significant, in semiconductors all the three hyperfine interactions are expected to be important.

In view of paucity of a systematic study of indirect nuclear hyperfine interactions in semiconductors we have decided to calculate the indirect nuclear ^{207}Pb spin-spin coupling tensor in both n-type and p-type PbTe, which are degenerate narrow-gap semiconductors. The degeneracy makes these semiconductors metal-like except that the carrier concentrations in these systems are a few orders of magnitude less than in metals. This, however, should not be viewed as a statement against the semiconducting characteristics of these systems. The other motivation is that we have in recent years investigated thoroughly some other hyperfine properties, such as the Knight shift and the chemical shift in PbTe, which show good agreement with experimental results where available.[11–13] Furthermore, indirect exchange interaction between localized magnetic impurities in semiconductors in-

cluding the one based on the lead salts have been of considerable interest[14–18] in recent years and furnish useful data regarding magnetic interactions in the diluted magnetic semiconductors that are considered as an interesting class of magnetic materials. This provides further motivation for seeing how the indirect exchange interactions involving nuclear spins are useful in probing the electronic structure in semiconductors vis-a-vis interactions involving magnetic impurities.

The paper is organized in the following manner. In Sec. II, we discuss the theory and the calculational procedure of the indirect exchange coupling constant between ^{207}Pb nuclear spins in PbTe. In Sec. III, we evaluate three types of contributions from (a) a full valence band and an empty conduction band, (b) electrons in n-type PbTe, and (c) holes in p-type PbTe. In Sec. IV we present our results and discuss them followed by our concluding remarks.

II. THEORY AND CALCULATIONAL PROCEDURE

A. Theory

The indirect nuclear interaction describes an interaction in which a nuclear magnetic moment with spin $\mathbf{I}_j$ at the lattice site $\mathbf{R}_j$ creates a local magnetic perturbation that induces an electronic magnetization varying in space, which in turn interacts with another nuclear moment of spin $\mathbf{I}_{j'}$ at the lattice site $\mathbf{R}_{j'}$. This results in a static coupling between the nuclear moments and is given by[10]

$$\mathcal{H}_{\rm int}=\sum_{j,j',(j\neq j')\cdot\mu,\nu} A^{\mu\nu}_{jj'} I^{\mu}_{j} I^{\nu}_{j'}, \tag{1}$$

where $A^{\mu\nu}_{jj'}$ is the indirect nuclear spin-spin coupling tensor and is given, in the presence of spin-orbit and electron-electron interactions, by

$$\begin{aligned} A^{\mu\nu}_{jj'}=\mu_0^2\mu_{0N}^2 g_{I_j} g_{I_{j'}} \sum_{n,n',\mathbf{k},\mathbf{k}'} & \frac{1}{1-\gamma_{n,n'}(\mathbf{k},\mathbf{k}')} \\ &\times[X^{\mu}_{n\mathbf{k}\rho,n'\mathbf{k}'\rho'} X^{\nu}_{n'\mathbf{k}'\rho',n\mathbf{k}\rho}\exp\{-i(\mathbf{k}-\mathbf{k}')\cdot\mathbf{R}_{ij'}\} \\ &+X^{\nu}_{n\mathbf{k}\rho,n'\mathbf{k}'\rho'} X^{\mu}_{n'\mathbf{k}'\rho',n\mathbf{k}\rho}\exp\{+i(\mathbf{k}-\mathbf{k}')\cdot\mathbf{R}_{jj'}\}] \\ &\times\frac{f(E_{n\mathbf{k}})}{E_{n\mathbf{k}}-E_{n'\mathbf{k}'}}. \end{aligned} \tag{2}$$

In Eq. (2), μ_0 and μ_{0N} are Bohr and nuclear magnetons, respectively; g_{I_j} and $g_{I_{j'}}$ are the nuclear g factors for the spins at $\mathbf{R}_j$ and $\mathbf{R}_{j'}$, respectively; $\mathbf{R}_{jj'}=\mathbf{R}_j-\mathbf{R}_{j'}$, γ denotes the exchange enhancement parameter due to the electron-electron interactions, and the electron-nuclear hyperfine vertex X^{μ} is given by

$$\begin{aligned} X^{\mu}&=\frac{8\pi}{3}\sigma^{\mu}\delta(\mathbf{r})+\left[-\frac{\sigma^{\mu}}{r^3}+\frac{3(\boldsymbol{\sigma}\cdot\mathbf{r})r^{\mu}}{r^5}\right]+2\epsilon_{\mu\nu\eta}\frac{r^{\nu}\pi^{\eta}}{\hbar r^3} \\ &\equiv X^{\mu}_{c}+X^{\mu}_{d}+X^{\mu}_{o}. \end{aligned} \tag{3}$$

The matrix elements of $\mathbf{X}$ are taken between the Bloch states $\psi_{n\mathbf{k}\rho}(\mathbf{r})$ and $\psi_{n'\mathbf{k}'\rho'}(\mathbf{r})$; the corresponding energies are $E_{n\mathbf{k}}$ and $E_{n'\mathbf{k}'}$, respectively. Here ρ and ρ' denote Kramer's conjugate pairs in the presence of spin-orbit interaction. $f(E_{n\mathbf{k}})$ is the Fermi function. In Eq. (3) the first term denotes the contact hyperfine vertex X^{μ}_{c}, the second term represents the dipolar hyperfine vertex X^{μ}_{d}, and the third describes the orbital hyperfine vertex $X^{\mu}_{o}\cdot\boldsymbol{\sigma}$ are the Pauli spin matrices and $\boldsymbol{\pi}$ is the electronic momentum operator in the presence of spin-orbit interaction. $\epsilon_{\mu\nu\eta}$ is an antisymmetric tensor of third rank and we follow the Einstein summation convention. Equation (2) in principle contains both oscillatory ($\mathbf{k}\neq\mathbf{k}'$) and nonoscillatory ($\mathbf{k}=\mathbf{k}'$) terms. The nonoscillatory terms are not of interest here as these are independent of $\mathbf{R}_{jj'}$. Hence we rewrite Eq. (2), considering only the oscillatory terms as

$$\begin{aligned} A^{\mu\nu}_{jj'}=&\sum_{\mathbf{k},n,\mathbf{k}',(\mathbf{k}\neq\mathbf{k}'),\rho,\rho'}\frac{1}{1-\gamma_{n,n}(\mathbf{k},\mathbf{k}')} \\ &\times[P^{\mu}_{jn\mathbf{k}\rho,n,\mathbf{k}'\rho'}P^{\nu}_{jn\mathbf{k}'\rho',n\mathbf{k}\rho}\exp\{-i(\mathbf{k}-\mathbf{k}')\cdot\mathbf{R}_{jj'}\} \\ &+P^{\nu}_{j'n\mathbf{k}\rho,n,\mathbf{k}'\rho'}P^{\mu}_{j'n\mathbf{k}'\rho',n\mathbf{k}\rho}\exp\{+i(\mathbf{k}-\mathbf{k}')\cdot\mathbf{R}_{ij'}\}] \\ &\times\frac{f(E_{n\mathbf{k}})}{E_{n\mathbf{k}}-E_{n\mathbf{k}'}} \\ &+\sum_{n,n'\mathbf{k},\mathbf{k}',(n\neq n'),(\mathbf{k}\neq\mathbf{k}'),\rho,\rho'}\frac{1}{1-\gamma_{n,n'}(\mathbf{k},\mathbf{k}')} \\ &\times[P^{\mu}_{jn\mathbf{k}\rho,n',\mathbf{k}'\rho'}P^{\nu}_{jn'\mathbf{k}',\rho',n\mathbf{k}\rho}\exp\{-i(\mathbf{k}-\mathbf{k}')\cdot\mathbf{R}_{jj'}\} \\ &+P^{\nu}_{j'n\mathbf{k}\rho,n',\mathbf{k}'\rho'}P^{\mu}_{j'n'\mathbf{k}'\rho',n\mathbf{k}\rho}\exp\{+i(\mathbf{k}-\mathbf{k}')\cdot\mathbf{R}_{jj'}\}] \\ &\times\frac{f(E_{n\mathbf{k}})}{E_{n\mathbf{k}}-E_{n'\mathbf{k}'}}, \end{aligned} \tag{4}$$

where

$$P^{\mu}_{j}=\mu_0\mu_{0_N}g_{I_J}X^{\mu}(\mathbf{r}), \tag{5}$$

$$\gamma_{nn}(\mathbf{k},\mathbf{k}')=-\sum_{\mathbf{k}'',\mathbf{k}'''}\overline{v}_{nn}(\mathbf{k},\mathbf{k}',\mathbf{k}'',\mathbf{k}''')\frac{f(E_{n\mathbf{k}''})-f(E_{n\mathbf{k}'''})}{E_{n\mathbf{k}''}-E_{n\mathbf{k}'''}} \tag{6}$$

and

$$\gamma_{nn'}(\mathbf{k},\mathbf{k}')=-\sum_{\mathbf{k}'',\mathbf{k}'''}\overline{v}_{nn'}(\mathbf{k},\mathbf{k}',\mathbf{k}'',\mathbf{k}''')\frac{f(E_{n\mathbf{k}''})-f(E_{n'\mathbf{k}'''})}{E_{n\mathbf{k}''}-E_{n'\mathbf{k}'''}}, \tag{7}$$

$\overline{v}$ being the average interparticle interaction. In Eq. (4) the first term describes the intraband Ruderman-Kittel-Kasuya-Yosida (RKKY) type of interactions and the second term describes the interband RKKY type of coupling. While in metals, it is a normal practice to consider the first term only, both of the terms are important in semiconductors. γ_{nn} and $\gamma_{nn'}$ are the intraband and the interband exchange enhancement parameters and are due to the electron-electron interactions in the same band and between bands, respectively.

B. Calculational procedure

PbTe is a narrow-gap semiconductor with a direct energy gap at the L point of the Brillouin zone. In addition to the band-edge states, there are two more bands on either side of the gap, which contributes to the effective mass formalism.

Each level is Kramer's split in the presence of spin-orbit interaction. The basis wave functions for all six levels and the energy gaps at the L points are taken from Mitchell and Wallis (MW).[19]

The Hamiltonian for the band-edge states is diagonalized exactly and the resulting states are treated with the far bands using second-order perturbation theory within a $\mathbf{k}\cdot\boldsymbol{\pi}$ formalism. The detailed mathematics of the procedure followed is given in our earlier publications[11–13] and we do not consider it essential to reproduce them here.

PbTe is a degenerate semiconductor implying thereby that the Fermi level, as in the metals, is in the allowed bands and is a function of carrier concentration. The Fermi surface of the carriers is ellipsoidal for low carrier concentrations and becomes cylindrical as the carrier density is increased. Thus the Fermi surface integrations that occur in both the evaluation of Fermi energy and the intraband and the interband coupling terms are carried out using a cylindrical coordinate system. The Fermi energies, as functions of electron and hole densities, respectively, in n- and p-type PbTe, are evaluated following a self-consistent method. The Fermi energies increase with increase in carrier density in both n- and p-type PbTe. However, this increase is not monotonic but tends to deviate from the linear behavior at higher carrier concentration, implying that the bands become nonparabolic because of the increasingly important effect of the far bands at this range of carrier concentrations.

For our calculations of the indirect exchange coupling tensor between ^{207}Pb nuclei, we have chosen X-, Y-, and Z-coordinate axes in the [112], [110], and [111] crystallographic directions, respectively. The nonzero hyperfine matrix elements at the L point of the Brillouin zone, using MW basis functions[19] are

$$\langle L_{61}^{+}\alpha|X_c^z|L_{61}^{+}\alpha\rangle=\frac{8\pi}{3}\cos^2\theta^{+}\langle R|\delta(r)|R\rangle=A_c^l, \quad (8)$$

$$\langle L_{62}^{-}\alpha|X_d^z|L_{62}^{-}\alpha\rangle=(\tfrac{4}{5}\sin^2\theta^{-}+\tfrac{2}{5}\cos^2\theta^{-})\times\left\langle X_+\left|\frac{1}{r^3}\right|X_+\right\rangle=A_d^l, \quad (9)$$

$$\langle L_{62}^{-}\alpha|X_o^z|L_{62}^{-}\alpha\rangle=2\cos^2\theta^{-}\left\langle X_+\left|\frac{1}{r^3}\right|X_+\right\rangle=A_o^l, \quad (10)$$

$$\langle L_{61}^{+}\alpha|X_c^x|L_{61}^{+}\beta\rangle=-A_c^l=A_c^t, \quad (11)$$

$$\langle L_{62}^{-}\alpha|X_d^x|L_{62}^{-}\beta\rangle=-\tfrac{1}{5}(2+4\cos^2\theta^{-}+3\sqrt{2}\sin\theta^{-}\cos\theta^{-})\times\left\langle X_+\left|\frac{1}{r^3}\right|X_+\right\rangle=A_d^t, \quad (12)$$

and

$$\langle L_{62}^{-}\alpha|X_o^x|L_{62}^{-}\beta\rangle=-2\sqrt{2}\sin\theta^{-}\cos\theta^{-}\left\langle X_+\left|\frac{1}{r^3}\right|X_+\right\rangle=A_o^t. \quad (13)$$

In Eqs. (8)–(13) $\cos\theta^{\pm}$ and $\sin\theta^{\pm}$ are the amplitudes of the single-group wave functions in the MW basis states. R transforms like an atomic s orbital around Pb. X_+ transforms like a atomic p orbital with $m_z=1$. The superscripts l and t represent longitudinal and transverse components, respectively. The above equations change sign when the matrix elements are considered by interchanging α and β. The equality in magnitude of A_c^l and A_c^t reflects the spatial isotropy of the contact hyperfine interaction. However, the orbital and the dipolar hyperfine matrix elements are anisotropic. It may be noted that in the absence of spin-orbit interactions the dipolar interactions become zero for crystals with cubic symmetry.

The **k**-dependent matrix elements are calculated using the wave functions of Eq. (7) of Ref. 12 for the band-edge states and the MW basis functions[19] for the other bands. The energy differences were evaluated using the conduction- and the valence-band energies derived earlier.[20]

III. EVALUATION OF $A(R)$

We evaluate $A(R)$ for three cases: for a full valence band and an empty conduction band, for n-type PbTe and for p-type PbTe. We evaluate both the longitudinal and the transverse components in each case. In case of the full band or the lattice contribution we assume the Brillouin zone to be divided into four equal spheres around each L point and the $\mathbf{k}$ and the $\mathbf{k}'$ integrations were performed using spherical polar coordinates. For carriers, either electrons or holes, we use cylindrical coordinates to evaluate the Fermi surface integrals for n- and p-type of PbTe. Following the procedure described in the preceding section, we obtain various contributions to $A_{jj'}$ for the full valence band, n-type PbTe and p-type PbTe as follows.

A. Full valence-band contribution to $A_{jj'}^{\mu\nu}$

For the full valence band, the intraband contribution is zero. Using Eqs. (4) and (8)–(13) and Eqs. (7) and (11) of Ref. 13, we obtain the interband contribution as

$$A_{fb}^l(R)=\frac{4C}{(2\pi)^4}\int_0^{k_0}dk_r\int_0^{k_0}dk_r'\int_0^{\pi}d\theta\int_0^{\pi}d\theta'\sin\theta\sin\theta' k_r^2 k_r'^2\times\cos[(k_r\cos\theta-k_r'\cos\theta')R]\times\left[\frac{Q_{\text{inter}}^l}{\frac{\hbar^2}{2m}(k_r^2-k_r'^2)-\frac{1}{2}E_g(W+W')}\right], \quad (14)$$

where

$$Q_{\text{inter}}^l=\left[\frac{(1+W)(\alpha\sin^2\theta'+\beta\cos^2\theta')k_r'^2(A_c^l)^2}{(1+W')}+\frac{(1+W')(\alpha\sin^2\theta+\beta\cos^2\theta)k_r^2(A_o^l+A_d^l)^2}{(1+W)}-2\beta k_r k_r'\cos\theta\cos\theta' A_c^l(A_o^l+A_d^l)\right]\frac{1}{WW'}. \quad (15)$$

Further,

$$W=(1+\alpha k_r^2 \sin^2\theta+\beta k_r^2\cos^2\theta)^{(1/2)} \tag{16}$$

and W' is same as W except that k_r and θ are replaced by k_r' and θ'; α and β are defined in our earlier work[20] and are expressed in terms of momentum matrix elements between band-edge states and the energy gap E_g at the L point. $C=\mu_0^2\mu_{0_N}^2 g_{I_j}^2$. The subscripts fb, intra, and inter stand for the full band, intraband, and interband contributions, respectively. k_0 is the radius of each sphere and the number 4 accounts for all the four valleys.

The transverse term $A_{\rm fb}^t(R)$ can be obtained by replacing A_c^l, A_d^l, and A_o^l by A_c^t, A_d^t, and A_o^t and changing the sign of the third term in Eq. (15).

B. Contributions due to electrons in *n*-type PbTe to $A_{jj'}^{\mu\nu}$

The electronic contributions in n-type PbTe to the oscillatory coupling constant is

$$A_e^l(R)=\frac{C}{(2\pi)^6}\int_0^{2\pi}d\phi\int_0^{2\pi}d\phi'\int_{-k_{l_e}}^{+k_{l_e}}dk_z\int_{-k_{l_e}'}^{+k_{l_e}'}dk_z'\int_0^{k_{\rho_e}^2}dk_\rho^2\int_0^{k_{\rho_e}'^2}dk_\rho'^2$$
$$\times\cos\left[(k_\rho\cos\phi+k_\rho\sin\phi+k_z-k_\rho'\cos\phi'-k_\rho'\sin\phi'-k_z')\frac{R}{\sqrt{3}}\right]$$
$$\times\left[\frac{Q_{e;\rm intra}^l}{\frac{\hbar^2}{2m}(k^2-k'^2)+\frac{1}{2}E_g(W-W')}+\frac{Q_{e;\rm inter}^l}{\frac{\hbar^2}{2m}(k^2-k'^2)+\frac{1}{2}E_g(W+W')}\right], \tag{17}$$

where

$$Q_{e;\rm intra}^l=\left[\frac{\{\alpha^2k_\rho^2k_\rho'^2+\beta^2k_z^2k_z'^2+\alpha\beta(k_\rho^2k_z'^2+k_\rho'^2k_z^2)\}}{(1+W)(1+W')}(A_c^l)^2\right.$$
$$\left.+(1+W)(1+W')(A_o^l+A_d^l)^2+2\{\beta k_zk_z'-\alpha k_\rho k_\rho'\cos(\phi+\phi')\}A_c^l(A_o^l+A_d^l)\right]\frac{1}{4WW'}, \tag{18}$$

and

$$Q_{e;\rm inter}^l=\left[\frac{(1+W)}{(1+W')}(\alpha k_\rho'^2+\beta k_z'^2)(A_o^l+A_d^l)^2+\frac{(1+W')}{(1+W)}(\alpha k_\rho^2+\beta k_z^2)(A_c^l)^2\right.$$
$$\left.-2\{\beta k_zk_z'-\alpha k_\rho k_\rho'\cos(\phi+\phi')\}A_c^l(A_o^l+A_d^l)\right]\frac{1}{4WW'}. \tag{19}$$

The transverse components $A_e^t(R)$ can be obtained as before by replacing A_c^l, A_d^l, and A_o^l by A_c^t, A_d^t, and A_o^t and changing the signs of the third terms in Eqs. (18) and (19).

C. Contributions due to holes in *p*-type PbTe to $A_{jj'}^{\mu\nu}$

The indirect nuclear coupling between ^{207}Pb spins in p-type PbTe can similarly be written as

$$A_h^l(R)=\frac{C}{(2\pi)^6}\int_0^{2\pi}d\phi\int_0^{2\pi}d\phi'\int_{-k_{l_h}}^{+k_{l_h}}dk_z\int_{-k_{l_h}'}^{+k_{l_n}'}dk_z'\int_0^{k_{\rho_h}^2}dk_\rho^2\int_0^{k_{\rho_h}'^2}dk_\rho'^2$$
$$\times\cos\left[(k_\rho\cos\phi+k_\rho\sin\phi+k_z-k_\rho'\cos\phi'-k_\rho'\sin\phi'-k_z')\frac{R}{\sqrt{3}}\right]$$
$$\times\left[\frac{Q_{h;\rm intra}^l}{\frac{\hbar^2}{2m}(k^2-k'^2)-\frac{1}{2}E_g(W-W')}+\frac{Q_{h;\rm inter}^l}{\frac{\hbar^2}{2m}(k^2-k'^2)-\frac{1}{2}E_g(W+W')}\right], \tag{20}$$

where

$$Q^l_{h;\text{intra}}=\left[\frac{\{\alpha^2k_\rho^2k_\rho'^2+\beta^2k_z^2k_z'^2+\alpha\beta(k_\rho^2k_z'^2+k_\rho'^2k_z^2)\}}{(1+W)(1+W')}(A^l_o+A^l_d)^2\right.$$
$$\left.+(1+W)(1+W')(A^l_c)^2+2\{\beta k_zk_z'-\alpha k_\rho k_\rho'\cos(\phi-\phi')\}A^l_c(A^l_o+A^l_d)\right]\frac{1}{4WW'} \quad (21)$$

and

$$Q^l_{h;\text{inter}}=\left[\frac{(1+W)}{(1+W')}(\alpha k_\rho'^2+\beta k_z'^2)(A^l_c)^2+\frac{(1+W')}{(1+W)}(\alpha k_\rho^2+\beta k_z^2)(A^l_o+A^l_d)^2\right.$$
$$\left.-2\{\beta k_zk_z'-\alpha k_\rho k_\rho'\cos(\phi-\phi')\}A^l_c(A^l_o+A^l_d)\right]\frac{1}{4WW'}. \quad (22)$$

The transverse components $A^t_h(R)$ can be obtained as before by replacing A^l_c, A^l_d, and A^l_o by A^t_c, A^t_d, and A^t_o and changing the signs of the third terms of Eqs. (21) and (22). k_{l_e} is obtained by solving the equation $E_c(k_\rho^2,k_z)=\mu$, where $E_c(k_\rho^2,k_z)$ is given by Eq. (3.2) of Ref. 20, for $k_\rho^2=0$. $k^2_{\rho_e}$ is obtained from the same equation self-consistently. Similar procedures were followed for obtaining k_{l_h} and $k^2_{\rho_h}$. μ is the Fermi energy and the procedure to obtain it is already discussed in the earlier section. The integrations occurring in Eqs. (14), (17), and (20) were performed numerically. In general, we use for the computation of the results

$$A=\tfrac{1}{3}A^l_\tau+\tfrac{2}{3}A^t_\tau, \quad (23)$$

where

$$A^{l,t}_\tau=A^{l,t}_{\tau,\text{intra}}+A^{l,t}_{\tau,\text{inter}}, \quad (24)$$

and τ stands for fb (full valence band), e (electrons), and h (holes), successively. We present our results and discuss them in the following section.

IV. RESULTS AND DISCUSSION

The oscillatory indirect nuclear spin-spin coupling constant is calculated for a number of values of R for a full valence band, results of which are presented in Table I. For low values of internuclei separation the coupling is negative and hence ferromagnetic (FM). This agrees with the prediction by Liu and Bastard[18] in case of indirect exchange interaction between magnetic impurities in PbTe. As the separation of the nuclei increases the indirect coupling constant changes from FM order to antiferromagnetic (AFM) order. From Table I, we see that all the three hyperfine interactions are very important. For example, if we consider only contact interaction the coupling tensor is significantly reduced as seen in the bottom portion of Table I. This is also reflected in Fig. 1. Since the valence band has predominantly atomic s character around lead (Pb) and the conduction band has p character, the significant change brought about by the orbital and the dipolar hyperfine interactions is due to the interband contributions arising out of mixing of the bands. The anisotropy reflected in the values is due to the effects of both dipolar and orbital hyperfine interactions. However, our calculation shows that the orbital anisotropy is very small compared to the dipolar anisotropy.

In Table II we have given the carrier contribution to the indirect nuclear coupling constant in p-type PbTe for two typical hole densities of 10^{17} cm^{-3} and 10^{18} cm^{-3}. As expected, the intraband contribution is dominant. However, with increase in carrier density the interband contribution increases and at a hole density of 10^{18} cm^{-3} it is still two orders less than the intraband contribution. Since the atomic orbitals around Pb transform in an s-type manner, the contact interaction is dominant and hence the coupling constant shows almost isotropic behavior. Up to a carrier density of 10^{18} cm^{-3} the orbital and the dipolar hyperfine interactions apparently have no effect on the coupling constant. $A_{jj'}$ decreases with the increase in internuclei separation, but never

TABLE I. Interband contributions to $A_{\text{fb}}(R)$ (all expressed in units of cps). Top: due to all three hyperfine interactions. Bottom: due to contact interaction alone.

R (Å)	A^l_{inter}	A^t_{inter}	A_{fb}
	Top		
6	−645.08	−867.99	−793.69
12	−480.93	−639.01	−586.32
18	−264.30	−342.22	−316.63
24	−52.52	−62.72	−59.32
30	114.18	149.21	137.54
36	221.45	281.59	261.85
42	274.87	348.75	324.12
48	287.11	368.46	341.34
54	268.54	350.03	322.86
60	225.43	296.87	273.06
	Bottom		
6	−371.13	−371.13	−371.13
12	−276.08	−276.08	−276.08
18	−153.88	−153.88	−153.88
24	−36.21	−36.21	−36.21
30	54.31	54.31	54.31
36	113.15	113.15	113.15
42	140.31	140.31	140.31
48	149.36	149.36	149.36
54	144.83	144.83	144.83
60	122.20	122.20	122.20

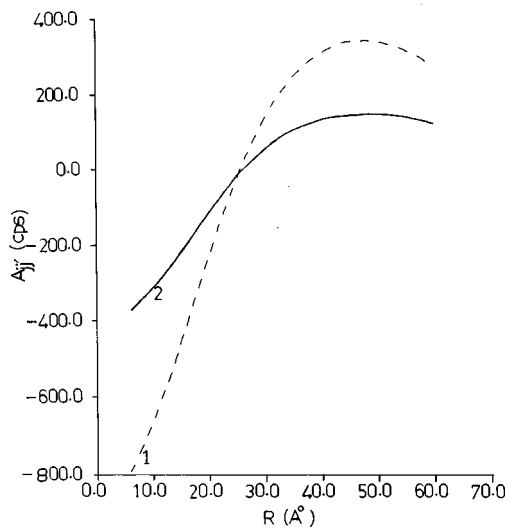

FIG. 1. $A_{jj'}$ for the full valence band and empty conduction band in PbTe as a function of R with all the three hyperfine interactions (1) and only the contact hyperfine interaction (2).

changes sign up to $R=60$ Å. Thus for all values of R considered the indirect nuclear spin-spin interaction due to holes is antiferromagnetic.

In Table III we have given the carrier contribution to the indirect nuclear spin-spin interaction for n-type PbTe for electron densities same as the hole densities. The coupling constant shows similar trend as in p-type PbTe. However, the magnitudes are higher by about 1.7 times for a carrier density of 10^{17} cm^{-3} and about three times for 10^{18} cm^{-3}.

TABLE II. Intraband and interband contributions to $A_h(R)$ (all expressed in units of 10^{-2} cps) for two typical hole densities.

p	R (Å)	A^l_{intra}	A^t_{intra}	A_{intra}	A^l_{inter}	A^t_{inter}	A_{inter}	A_h
				10^{17} cm^{-3}				
	6	2.65	2.63	2.64	0.00085	0.00169	0.00141	2.64
	12	2.66	2.64	2.65	0.00110	0.00211	0.00177	2.65
	18	2.66	2.64	2.64	0.00109	0.00209	0.00176	2.65
	24	2.65	2.63	2.64	0.00108	0.00207	0.00174	2.64
	30	2.64	2.62	2.63	0.00106	0.00204	0.00171	2.63
	36	2.63	2.61	2.62	0.00104	0.00200	0.00168	2.62
	42	2.61	2.00	2.60	0.00102	0.00195	0.00164	2.60
	48	2.60	2.58	2.59	0.00099	0.00190	0.00159	2.59
	54	2.58	2.57	2.57	0.00095	0.00184	0.00155	2.57
	60	2.57	2.55	2.56	0.00092	0.00178	0.00149	2.56
				10^{18} cm^{-3}				
	6	57.15	55.46	56.02	0.299	0.596	0.497	56.52
	12	56.94	55.27	55.82	0.297	0.592	0.493	56.32
	18	56.59	54.95	55.50	0.294	0.585	0.488	55.98
	24	56.10	54.51	55.04	0.289	0.576	0.481	55.52
	30	55.47	53.95	54.46	0.284	0.565	0.471	54.93
	36	54.72	53.27	53.76	0.277	0.552	0.460	54.22
	42	53.84	52.49	52.94	0.269	0.536	0.447	53.39
	48	52.85	51.60	52.02	0.260	0.519	0.433	52.45
	54	51.75	50.61	50.99	0.251	0.499	0.417	51.40
	60	50.54	49.52	49.86	0.240	0.479	0.399	50.26

Since the conduction-band wave functions in PbTe transform like the atomic p orbital around Pb, the orbital and the dipolar hyperfine interactions are dominant for n-type PbTe. It has also been observed that neglect of contact hyperfine interaction for n-type PbTe up to 10^{18} cm^{-3} does not affect the results in a significant way. However, neglect of either orbital or dipolar hyperfine interactions drastically affects the results. Thus in n-type PbTe the noncontact interactions are found to be dominant. Furthermore, significant anisotropy seems to be present in case of n-type PbTe.

Unfortunately, we have not encountered any experimental results to compare with our results. However, a qualitative comparison can be made. The indirect nuclear coupling constant has been measured[21] in the case of metallic lead. The RK coupling constant for nearest neighbors is 4800 ± 500 cps. This value is approximately more than four orders of magnitude higher than the indirect nuclear coupling constant calculated for an electron density of 10^{18} cm^{-3}. We see from Table III that $A_{jj'}$ increases by one order when we increase the electron density from 10^{17} cm^{-3} to 10^{18} cm^{-3}. Therefore, we believe that the difference in magnitudes of $A_{jj'}$ for the electron density of 10^{18} cm^{-3} in n-type PbTe and in metallic Pb is reasonable. It would be pertinent to compare features observed in our calculation with that observed in metals. In metals, the oscillations are rapid and have a pronounced decay. However, we do not see such features here. This is due probably to the fact here the **k**-space integration is confined to a small region around the L point of the Brillouin zone. Indeed the effective mass approximation involving the Luttinger-Kohn basis sets[22] followed in the calculation is valid only for **k** values not far from $\mathbf{k}_0$ (here the L point). In contrast, in metals the **k** summation covers the entire **k** space. At higher concentrations of carriers the calculations might show features as observed in metals. However, our model does not work well beyond a carrier density of 10^{18} cm^{-3}. It may also be noted that the importance of anisotropic noncontact hyperfine interactions seen in our calculations is not an exception. Anisotropic indirect spin-spin coupling and experimental evidence[23] of noncontact contributions to $A_{jj'}$ have been observed between ^{31}P-^{199}Hg for a series of mercury phosphines $[HgPR_3(NO_3)]_2$, where R is either an alkyl or an aryl group.

In conclusion, we would like to state that we have made a careful analysis of various contributions to the indirect nuclear spin-spin coupling tensor in PbTe. The calculations take into account all the three types of hyperfine interactions and include both intraband and interband contributions. The relativistic effects are considered through the double group basis wave functions and energy levels. The coupling tensor for a full valence band is quite appreciable and changes from FM to AFM order as the nuclear separation increases. We have also calculated the carrier (both holes and electrons) contributions to $A_{jj'}$ for two typical carrier densities in each case. The carrier contributions, as expected, are much smaller than the full band contribution in the range of carrier densities considered. This also agrees with the prediction in case of indirect exchange interactions involving magnetic impurities[18] in PbTe. In case of p-type PbTe the contact interaction was found to be dominant. However, for n-type PbTe, the orbital and the dipolar hyperfine interactions are found to be important. The differences are attributed to the

TABLE III. Intraband and interband contributions to $A_e(R)$ (all expressed in units of 10^{-2} cps) for two typical electron densities.

n	R (Å)	A^l_{intra}	A^t_{intra}	A_{intra}	A^l_{inter}	A^t_{inter}	A_{inter}	A_e
				10^{17} cm^{-3}				
	6	3.13	5.16	4.48	0.00082	0.00166	0.00138	4.48
	12	3.20	5.28	4.59	0.00108	0.00207	0.00174	4.59
	18	3.19	5.27	4.58	0.00107	0.00205	0.00173	4.58
	24	3.18	5.26	4.56	0.00106	0.00203	0.00171	4.56
	30	3.16	5.24	4.55	0.00104	0.00200	0.00168	4.55
	36	3.15	5.21	4.52	0.00101	0.00195	0.00164	4.52
	42	3.13	5.18	4.49	0.00098	0.00190	0.00160	4.49
	48	3.11	5.14	4.46	0.00095	0.00185	0.00155	4.46
	54	3.08	5.10	4.43	0.00092	0.00178	0.00150	4.43
	60	3.05	5.06	4.39	0.00088	0.00172	0.00144	4.39
				10^{18} cm^{-3}				
	6	113.1	183.0	159.7	0.291	0.589	0.489	160.2
	12	112.7	182.4	159.1	0.290	0.585	0.486	159.6
	18	112.0	181.4	158.3	0.286	0.578	0.481	158.7
	24	111.1	180.0	157.1	0.282	0.568	0.473	157.6
	30	109.9	178.2	155.4	0.276	0.556	0.463	155.9
	36	108.5	176.0	153.5	0.268	0.542	0.451	154.0
	42	106.8	173.5	151.3	0.260	0.526	0.438	151.7
	48	104.9	170.6	148.7	0.251	0.508	0.422	149.1
	54	102.8	167.3	145.8	0.241	0.488	0.406	146.2
	60	100.5	163.7	142.4	0.230	0.467	0.388	142.8

different kinds of transformations of the atomic wave functions around Pb in the valence and conduction bands. $A_{jj'}$ for a carrier density of 10^{18} cm^{-3} in n-type PbTe is found to be about four orders less than the corresponding value in metallic lead, which is justified in view of the fact that metallic density is about five orders higher than the maximum carrier density considered here. The present calculation also shows the importance of the noncontact hyperfine interactions in the calculation of the indirect nuclear coupling tensor. The calculation, we believe, is the first of its kind in semiconductors. We have not considered the core-polarization effects because it, being an intra-atomic phenomenon and weak in metallic lead, would not be significant in the present analysis.

ACKNOWLEDGMENTS

This research was supported by the Department of Science and Technology, Government of Orissa and partly by the CSIR (India). We are grateful to Dr. R. Sahu for making available to us his personal computer facilities.

[1] M. A. Ruderman and C. Kittel, Phys. Rev. **96**, 99 (1954).
[2] N. Bloembergen and T. J. Rowland, Phys. Rev. **97**, 1679 (1955).
[3] J. Poitrenaud, J. Phys. Chem. Solids **28**, 161 (1967).
[4] R. F. Walstedt, M. W. Dowley, E. L. Hahn, and C. Froidevaux, Phys. Rev. Lett. **8**, 406 (1962).
[5] L. Tterlikkis, S. D. Mahanti, and T. P. Das, Phys. Rev. **178**, 630 (1969).
[6] L. Tterlikkis, S. D. Mahanti, and T. P. Das, Phys. Rev. Lett. **21**, 1796 (1968).
[7] P. A. Lindgard, X. W. Wang, and B. N. Harmon, J. Magn. Magn. Mater. **54-57**, 1052 (1986); S. J. Frisken and D. J. Miller, Phys. Rev. Lett. **57**, 2971 (1986); **61**, 1017 (1988); A. S. Oja, X. W. Wang, and B. N. Harmon, Phys. Rev. B **39**, 4009 (1989).
[8] M. T. Huiku, T. A. Jyrkkio, J. M. Kyynarainen, M. T. Loponen, O. V. Lounasmaa, and A. S. Oja, J. Low Temp. Phys. **62**, 433 (1986).
[9] A. S. Oja and O. V. Lounasmaa, Rev. Mod. Phys. **69**, 1 (1997).
[10] G. S. Tripathi, Phys. Rev. B **31**, 5143 (1985).
[11] G. S. Tripathi, L. K. Das, P. K. Misra, and S. D. Mahanti, Phys. Rev. B **25**, 3091 (1982); S. Misra, G. S. Tripathi, and P. K. Misra, Phys. Lett. A **110**, 461 (1985); J. Phys. C **20**, 277 (1987).
[12] C. M. Misra and G. S. Tripathi, Phys. Rev. B **40**, 11 168 (1989); R. L. Hota and G. S. Tripathi, *ibid.* **44**, 1918 (1991).
[13] R. L. Hota, R. C. Patnaik, G. S. Tripathi, and P. K. Misra, Phys. Rev. B **51**, 7291 (1995).
[14] V. C. Lee and L. Liu, Phys. Rev. B **29**, 2125 (1984).
[15] S. J. Frisken and D. J. Miller, Phys. Rev. B **33**, 7134 (1986).
[16] S. S. Yu and V. C. Lee, Phys. Rev. B **40**, 10 621 (1989).
[17] A. D. Margulis and V. A. Margulis, Fiz. Tverd. Tela (Leningrad) **33**, 1531 (1991) [Sov. Phys. Solid State **33**, 863 (1991)].

[18] L. Liu and G. Bastard, Phys. Rev. B **25**, 487 (1982).
[19] D. L. Mitchell and R. F. Wallis, Phys. Rev. **151**, 581 (1966).
[20] R. L. Hota, G. S. Tripathi, and J. N. Mohanty, Phys. Rev. B **47**, 9319 (1993).
[21] H. Alloul and C. Froidevaux, Phys. Rev. **163**, 324 (1967).
[22] J. M. Luttinger and W. Kohn, Phys. Rev. **97**, 869 (1958).
[23] W. P. Power, M. D. Lumsden, and R. E. Wasylishen, J. Am. Chem. Soc. **113**, 8257 (1991).